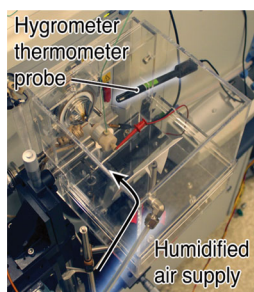


RESEARCH ARTICLE

Humidity Effects on Fragmentation in Plasma-Based Ambient Ionization Sources

G. Asher Newsome,¹ Luke K. Ackerman,² Kevin J. Johnson³¹Nova Research, Inc., 1900 Elkin St. Suite 230, Alexandria, VA 22308, USA²US-FDA Center for Food Safety and Applied Nutrition, Office of Regulatory Science - Division of Analytical Chemistry, 5100 Paint Branch Parkway, College Park, MD 20740, USA³US Naval Research Laboratory, Naval Technical Center for Safety and Survivability, Code 6180, 4555 Overlook Ave. SW, Washington, DC 20375, USA

Abstract. Post-plasma ambient desorption/ionization (ADI) sources are fundamentally dependent on surrounding water vapor to produce protonated analyte ions. There are two reports of humidity effects on ADI spectra. However, it is unclear whether humidity will affect all ADI sources and analytes, and by what mechanism humidity affects spectra. Flowing atmospheric pressure afterglow (FAPA) ionization and direct analysis in real time (DART) mass spectra of various surface-deposited and gas-phase analytes were acquired at ambient temperature and pressure across a range of observed humidity values. A controlled humidity enclosure around the ion source and mass spectrometer inlet was used to create programmed humidity and temperatures. The relative abundance and fragmentation of molecular adduct ions

for several compounds consistently varied with changing ambient humidity and also were controlled with the humidity enclosure. For several compounds, increasing humidity decreased protonated molecule and other molecular adduct ion fragmentation in both FAPA and DART spectra. For others, humidity increased fragment ion ratios. The effects of humidity on molecular adduct ion fragmentation were caused by changes in the relative abundances of different reagent protonated water clusters and, thus, a change in the average difference in proton affinity between an analyte and the population of water clusters. Control of humidity in ambient post-plasma ion sources is needed to create spectral stability and reproducibility.

Keywords: Humidity, FAPA, DART, Ambient ionization, Water cluster, Mechanism, Fragmentation

Received: 14 May 2015/Revised: 1 July 2015/Accepted: 22 August 2015/Published Online: 18 September 2015

Introduction

Many techniques have been developed recently for ambient ionization mass spectrometry, which allows rapid, real-time analysis with no sample pretreatment [1, 2]. Atmospheric pressure chemical ionization (APCI) describes ambient ionization with protons, reagent ions, electrons, or metastable atoms generated by a corona discharge or a plasma at atmospheric pressure [3]. In plasma-based APCI techniques, referred to as ambient desorption/ionization (ADI) [4], analytes are not directly exposed to the electrical discharge but rather to

the flow of ions and energetic species produced by it [5–11]. Post-plasma flow is directionally controlled, allowing the ionizing stream to impinge on solids and surfaces placed in the flow path before the MS inlet. Gaseous analyte in the flow path is also sampled as in corona discharge APCI. Post-plasma sources in the form of a probe are also readily used in open air for portable or fieldable mass spectrometry trace detection systems [12].

The various plasma-based ADI methods are distinguished by characteristics such as the means of plasma generation, temperature, and types of reagent ions [13]. The ionization techniques also share certain commonalities. All post-plasma ADI techniques that sample surfaces are thought to thermally desorb analytes. Several discharge gases have been tested and helium yielded good sensitivity for a range of analytes [14]. It is proposed that metastable helium from the plasma directly ionizes analytes via Penning ionization [6] and atmospheric

Electronic supplementary material The online version of this article (doi:10.1007/s13361-015-1259-y) contains supplementary material, which is available to authorized users.

Correspondence to: G. Newsome; e-mail: graham.newsome.ctr@nrl.navy.mil

gases to form reagent ions. Penning ionization and charge transfer reagents, chiefly protonated water, ionize analytes and yield a protonated water cluster background [14–16]. Commonly observed analyte species include the protonated molecule (MH^+), molecular ion (M^{++}), and related ions.

The importance of ambient humidity for ADI and corona discharge APCI methods is not generally acknowledged in literature, other than water vapor as a proton source [17, 18]. It has been implied for direct analysis in real time (DART) ionization that under typical ambient conditions water cluster formation is sufficiently rapid [6] to have no effect on ambient mass spectra. However, several research groups have used supplementary water with corona discharge APCI [19–22] to increase analyte MH^+ abundance. Large effects on mass spectra were also observed with DART of one analyte in a range of humidity values [23]. Humidity effects on another post-plasma ADI source, flowing atmospheric pressure afterglow (FAPA) ionization, were examined using saturated salt solutions to humidify nitrogen (or argon) in a cell sealing the FAPA directly to the mass spectrometer inlet [24]. However, most ADI analysis is performed with the post-plasma probe mounted in open laboratory air in front of the MS inlet (i.e., not a chemically modified atmosphere enclosure). In outdoor settings, ambient humidity is not controlled, but indoor humidity also fluctuates substantially because it is directly dependent on the operation of building temperature controls and ambient air source. Post-plasma ADI applications require a more comprehensive and user-relevant study of humidity effects to better understand limitations on reproducibility. The present work systematically examines and seeks to explain humidity effects on the relative ion abundance and reproducibility of post-plasma ADI mass spectra using FAPA and DART ion sources operating in the laboratory air.

For generated humidity experiments, an enclosure around the ion source and MS inlet was used to supply and regulate humidity. The amount of water vapor in air is most commonly expressed as percent relative humidity (RH):

$$RH\% = \frac{P_w}{P_{ws}} \times 100 \quad (1)$$

where P_w is the water vapor pressure in pascal, and P_{ws} is the saturation water vapor pressure in pascal at a given temperature. Air temperature may vary apart from relative humidity, and mass spectra acquired at constant relative humidity cannot necessarily be acquired at constant temperature (and P_{ws}) under ambient conditions at different times. Absolute humidity (AH) in g/m^3 is more descriptive of ambient conditions for the purposes here and is calculated according to:

$$AH = C \cdot \frac{RH \times P_{ws}}{T} \quad (2)$$

where C is a constant in gK/J and T is temperature in K [25, 26]. Various compounds were analyzed to observe the humidity dependence of mass spectra in terms of ratios

between observed ions and percent fragmentation of molecular adduct ions,

$$\% \text{ fragmentation} = 100 \times \frac{\sum_i F_i}{M + \sum_i F_i} \quad (3)$$

where M is total abundance of the intact molecular adduct ion(s) and F is the abundance of each fragment ion originating from the intact molecular adduct ion(s).

Methods

Analytes

Ultra high purity helium (5.0 grade; Airgas, Radnor, PA, USA) was used for both ion sources. Analytes were chosen to provide a variety of molecular adduct ions by different mechanisms. Propazine was obtained from the US Environmental Protection Agency, National Pesticide Standard Repository (Ft. Meade, MD, USA) and diluted to 100 ppm in acetonitrile. Analytical grade nicotine, limonene, ferrocene, and saffrole were purchased from Sigma (St. Louis, MO, USA) and diluted to 200 ppm in acetonitrile. HMTD was obtained from the FBI Explosives Unit (Quantico, VA, USA) in static-free vials containing a maximum of 0.5 g solids, stored within an MK663 blasting cap container (Camtech Precision Manufacturing, Inc., Auburn, NY, USA). With laboratory surfaces and personnel electrically grounded, and with no lightning within 30 nautical miles of the laboratory presently or within prior 2 h, HMTD was diluted to 80 ppm in acetonitrile behind a blast shield certified to a net explosives weight of 1.5 g. Solids and solutions were stored at -40°C .

Instrumentation and Data Analysis

Post-plasma ADI sources were mounted in front of the ion inlet of an LTQ Orbitrap XL mass spectrometer (Thermo Fisher Scientific, Waltham, MA, USA). A FAPA discharge cell with pin-to-capillary geometry [27] was held in position by a shaft collar, itself mounted on a rod extending from an xyz translation stage through a slot in the enclosure. The FAPA capillary was positioned 5 mm from the MS ion inlet for best signal intensity. A negative potential from a high-voltage power supply (Spellman SL600; Hauppauge, NY, USA) was applied across a 5 k Ω resistor to the cathode pin, and the power supply ground was connected to the anode capillary. Helium flow through the discharge cell was regulated with a calibrated mass flow controller (Sierra Smart-Tek 2; Monterey, CA, USA) and set to 0.7 L/min for positive mode analyses. Operating the discharge at a current-controlled 25 mA over an inter-electrode distance of 6.5 mm resulted in a voltage of 600 V. The MS inlet capillary was operated at 275°C and 38 V with a 100 V tube lens. Pressure measured by the LTQ ion gauge was 2.4×10^{-5} Torr during FAPA operation.

A DART-SVP with Vapur interface (IonSense, Saugus, MA, USA) was alternately mounted in front of the MS ion

inlet. The DART was positioned on-axis with the MS and Vapur inlets and ~2 cm from the Vapur's 1 cm i.d. ceramic transfer tube. The DART SVP was operated in positive mode with the helium discharge heated to 150–450°C, controlled by software. The differential membrane pump for the Vapur interface was adjusted until the LTQ ion gauge was at or below 2.4×10^{-5} Torr. The MS inlet capillary was operated at 200°C and 38 V with a 100 V tube lens. With both ion sources Orbitrap mass spectra were collected with a 25 ms maximum inject time. Data were extracted from .raw files for integration of profile mode ion signals.

Analytes were introduced to the ionization region by mounting sample surfaces in front of the discharge or by elution from a gas chromatograph (GC). Compounds in bulk solution were spotted onto laboratory tissue and allowed to dry, leaving analyte deposits on the order of ng/mm². The sample paper was mounted in front of ion sources orthogonal to the flow and positioned by an *xyz* translation stage so that the edge of the paper intersected the flow path.

The GC (Hewlett-Packard HP5890; Palo Alto, CA, USA) was operated at 1.5 mL/min helium flow through the column with a 10:1 split at the injector. Sample aliquots of 1 µL were injected at 250°C. After an initial 1 min hold time and temperature of 35°C, the GC oven was ramped at 1°C/min to 250°C. The end of the 15 m, 0.25 mm i.d. Restek RTX-5MS column was joined to a 1 m, 0.25 mm i.d. deactivated glass transfer capillary, which was passed out of the GC oven through an extension arm independently heated to 100°C. The end of the transfer capillary exiting the extension arm was wrapped with 30 AWG silver-coated copper wire and inserted snugly into 0.159 cm copper transfer tubing. The transfer tubing was itself independently heated to 70°C and mounted on an *xyz* translation stage. The layers wrapped around the transfer capillary ensured uniform heat transfer for good peak shape, and the mount telescoping the transfer tubing into the GC extension arm allowed the capillary to be manipulated when inside the enclosure. The end of the capillary was positioned at the midpoint between the ion source and mass spectrometer inlet to direct the analyte stream into the plasma afterglow.

HMTD and propazine were analyzed from surface deposits because of their low vapor pressure. Because of the difficulty in reproducibly-creating and reproducibly-desorbing from surface analyte deposits, relative ion abundance between intact and fragment ions in mass spectra was compared to normalize these random factors in overall signal abundance. Data from analytes introduced by GC was presented in the same way to facilitate comparison of humidity effects. Ion ratios were acquired from mass spectra of each ADI sampling of 2–8 s GC transients or 20–60 s of an analyte from a surface. Experiments were designed with masses of analytes well above intact adduct ion detection limits in order to ensure that low-abundance fragment ions would be identified for calculation of percent fragmentation. Mass scans were acquired with the Orbitrap analyzer from *m/z* 50 to analyte mass plus ~50 Da.

Humidity Control

A humidity control enclosure was designed to mate to the instrument housing around the ion inlet and fabricated from 3.2 mm-thick acrylic sheets (California Quality Plastics). The design consisted of a 20 cm cube with one open face joined to a frame in contact with the instrument housing. The interface to the housing was not sealed airtight but reinforced with tape at select points where the housing had a degree of curve. The enclosure was supported from below by table mounts. The upper portion of the enclosure was removable to allow placement of sample surfaces or to allow installation of the IonMax ESI source for periodic instrument calibration. Prior to use with an ion source, the enclosure was allowed to outgas from materials used in its construction and mounting. Duplicate enclosures were made to fit the FAPA and the DART cell and translation stage.

The enclosure contained feedthroughs for atmosphere sensors, ion source mounts, gas and electronic supplies, and analyte introduction. Air from a test atmosphere generator (Miller-Nelson HCS-501-50; Assay Technology, Livermore, CA, USA) at a flow rate of 23 L/min was supplied by 0.22 m of room-temperature Teflon tubing to an elbow fitting mounted to a corner of the enclosure opposite the ion inlet. A 10 × 7 cm baffle was positioned 4 cm from the supply port (11 cm for DART) to aid in mixing within the enclosure. The enclosure was not vacuum-sealed, and air was allowed to escape at the edges of the MS housing interface and the feedthroughs. Ambient pressure was maintained as measured by a pressure transducer (Omegadyne model PX309-015GV; Sunbury, OH, USA) when the test atmosphere flow was on. A thermohygrometer probe (Testo model 625; Sparta, NJ, USA) was mounted inside the enclosure 5 cm lateral to the MS ion inlet or ceramic ion inlet to the Vapur interface. Relative humidity and temperature were recorded during every analyte spectrum acquisition.

FAPA mass spectra were acquired over several months without the atmosphere enclosure in a laboratory with variable ambient humidity levels and temperatures. FAPA and DART mass spectra were also acquired with the ion source and analytes inside the atmosphere enclosure. Both the heated ion inlet and the ion sources were significant sources of heat, creating a gradient of temperature and humidity within the enclosure. The discharge was turned on and off apart from analysis time to stabilize the temperature and humidity. Temperature and humidity values were recorded at a constant position by the thermohygrometer. Humidity in the enclosure was adjusted by changing the settings of the test atmosphere generator, and it was allowed to stabilize for several min before analysis. Mass spectra of each analyte (at various enclosure humidity values) were acquired consecutively with the Orbitrap over a maximum temperature range of 1.7°C (2.0°C range for DART spectra). FAPA and DART mass spectra of reagent water cluster ions in the absence of analyte were acquired consecutively with the LTQ scanning *m/z* 15–140 over a maximum temperature range of 1.5°C. Because the

chamber was not vacuum-sealed to the instrument housing, external ambient conditions limited the accessible humidity range of the enclosure. Higher ambient humidity raised base humidity in the enclosure, increasing both the maximum and minimum achievable enclosure humidity.

The DART discharge gas temperature can be heated, and DART spectra were acquired at 150–350°C discharge gas. The recommended operating conditions for DART are 30%–70% relative humidity at 10–32.2°C [18], a total absolute humidity range of 2.8–24.0 g/m³. All analyses using the enclosure were performed within the recommended absolute humidity range and near the upper temperature limit of the DART source. Analyses performed with the enclosure below ~10 g/m³ were below the recommended relative humidity range but were representative of a common condition in many laboratories.

Results and Discussion

Over the course of one year, relative humidity levels were recorded from 7%–56% at 21–29°C, an absolute humidity range of 1.3–16 g/m³. With variations in local weather, laboratory relative humidity was observed to change up to ±15% between consecutive days and up to ±5% over the course of a single day. Enclosure humidity was tuned to stable values within a similar range.

Adjusting the enclosure humidity for FAPA and DART analysis produced no observably significant change in the abundance of protonated water clusters, with the exception of [(H₂O)₂H]⁺ (Figure 1). Other water cluster ions also had lower signal abundance than the proton-bound dimer, indicating that the latter is at least a significant reagent ion. The abundance of *m/z* 55 was increased by constant background signal from C₄H₇⁺ and C₃H₃O⁺ that was isobaric with the water trimer in this experiment. Any change in protonated trimer abundance with humidity was sufficiently minor so as to be obscured by background. DART used a different interface with the ion inlet

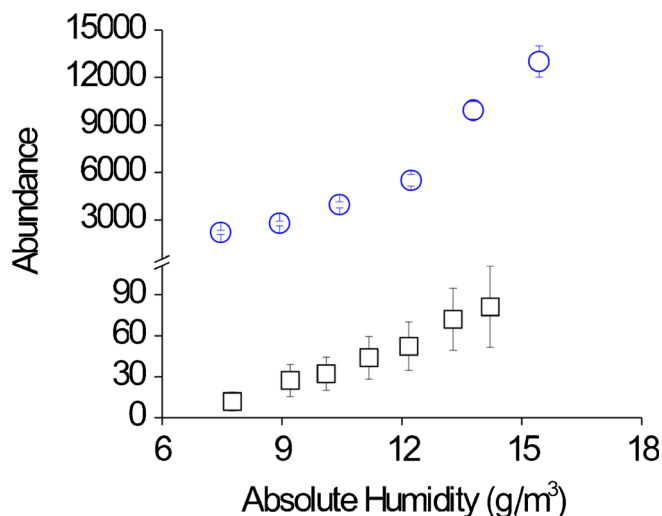


Figure 1. Signal from protonated water dimer [(H₂O)₂ + H]⁺ with FAPA (blue ○) and 150°C DART ionization (□) (± one SD)

and produced lower water cluster ion signal than FAPA. Similarly, water cluster variance with humidity differed slightly from previous observations with different experimental conditions and entrance optics [24]. The proton affinity of a water cluster increases with size (*n* = 1, 696 kJ/mol; *n* = 2, 833 kJ/mol; *n* = 3, 889 kJ/mol; *n* = 4, 920 kJ/mol; etc.) [28]. Proton affinity values of molecules similar to those studied range from 857–1055 kJ/mol (Online Resource 1). As humidity around the ion source increased and [(H₂O)₂H]⁺ rose in abundance, less exothermic proton transfer from the dimer increased relative to transfer from the monomer, and fragmentation decreased (Figures 1, 2, and 3).

FAPA Mass Spectra of Analytes as a Function of Humidity

The most abundant HMTD ions in the FAPA spectra were MH⁺ at *m/z* 209, two fragment ions of MH⁺ at *m/z* 179 and 145,

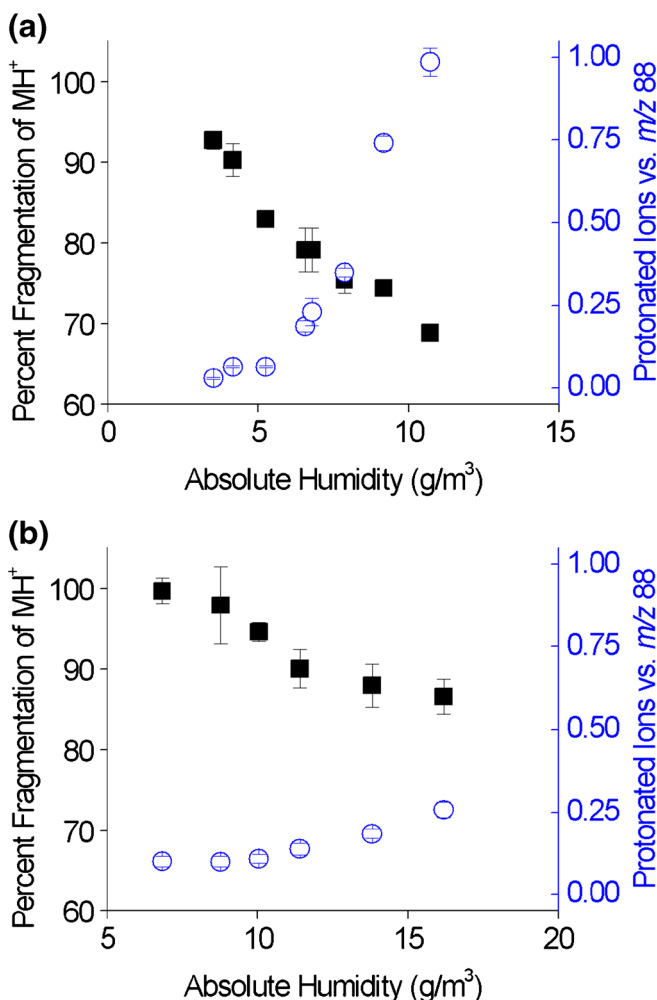


Figure 2. FAPA signal from HMTD with variation of (a) ambient humidity at 23–25°C and (b) enclosure humidity at 31.5–32°C, shown as percent fragmentation of protonated molecule (■) and ratio of protonated molecule plus fragment ions to M^{•+} fragment ions (blue ○) (± one SD)

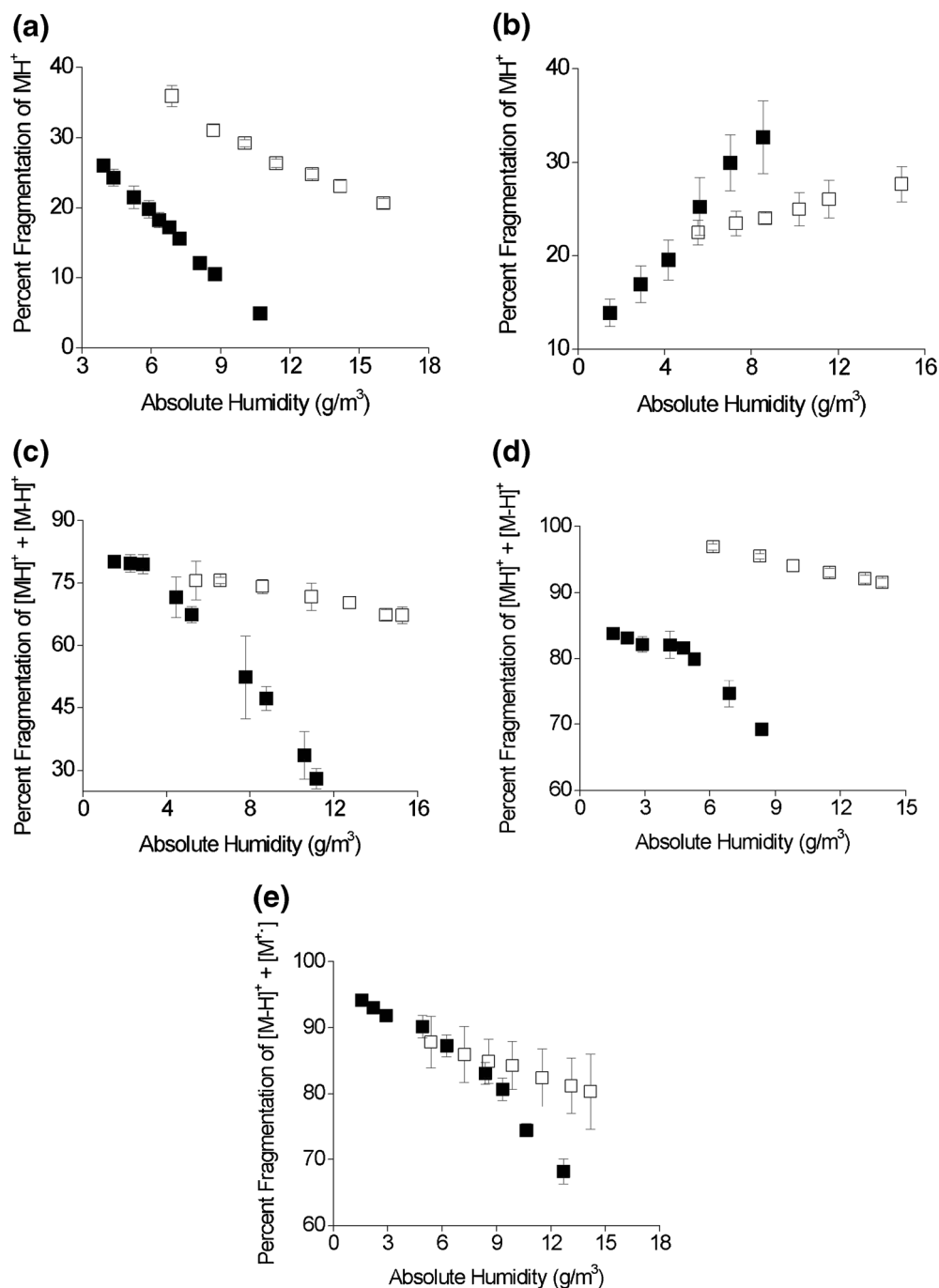


Figure 3. FAPA signal from (a) propazine, (b) ferrocene, (c) nicotine, (d) limonene, and (e) safrole, with variation of ambient humidity at 21–30°C (■) and enclosure humidity at 31.5–37°C (□), shown as percent fragmentation of protonated molecule (a), (b); protonated molecule and net deprotonated molecule (c), (d); and net deprotonated molecule and molecular ion (e) (\pm one SD)

and a radical fragment ion at m/z 88 as the base peak (Online Resource 2). The fragmentation of HMTD decreased when humidity increased, as shown by the changing ratio of protonated fragment ions to protonated molecule in Figure 2. More dramatically, the ratio between all protonated ions and the radical fragment ion (m/z 88) increased with increasing humidity. The result is a striking change in the FAPA spectra of HMTD between low and high humidity. The fragmentation effect was observed from ambient laboratory air humidity

changes (Figure 2a) and experimentally adjusting enclosure humidity (Figure 2b). Protonated molecule fragmentation was greater when the source was operated in the humidity enclosure versus the ambient laboratory air (at equal humidity values). Energy transfer from elevated temperature in the enclosure likely caused an increased baseline fragmentation that lowered the slope of fragmentation dependence on humidity. The inverse relationships with humidity and post-sample proton introduction are consistent with

competitive ionization mechanisms between the HMTD radical and protonated species.

Propazine was also analyzed by FAPA from a surface deposit, yielding the monoisotopic protonated molecule at m/z 230 and two fragment ions (Online Resource 3). The fragmentation was similarly observed to decrease with increasing humidity (Figure 3a). Like HMTD, MH^+ fragmentation was increased in the enclosure compared to ambient at equal humidity values. The slope of humidity dependence in the enclosure at elevated temperature was nearly identical to the slope of humidity dependence in ambient laboratory air conditions.

Analytes were also introduced via GC in order to observe humidity effects on fragmentation absent energy required for thermal desorption. Ferrocene eluted from a GC column produced M^{++} as the base peak, MH^+ , and fragment ions of protonated molecule (Online Resource 4). Unlike HMTD and propazine, the percent fragmentation of ferrocene MH^+ was observed to increase instead of decrease with greater ambient and enclosure humidity (Figure 3b). Proton transfer/abstraction followed by decomposition from excess energy was likely not the dominant mechanism for the formation of the principal fragment ion from ferrocene, $[C_5H_5Fe + H_2O]^+$ at m/z 139. Exchange of one cyclopentadienyl ring for water became increasingly favorable as humidity increased. The slope of the humidity dependence was also decreased by the elevated temperatures in the enclosure that make the water exchange more favorable at lower humidity. The ratio of MH^+ plus fragment ions to M^{++} was not significantly changed by humidity variation because humidity does not directly affect Penning ionization for ferrocene.

Nicotine and limonene introduced via GC both produced MH^+ , net deprotonated molecule ($[M - H]^+$), fragment ions, and related larger mass adduct ions including hydrated ions (Online Resources 5-6). The total percent fragmentation of MH^+ and $[M - H]^+$ was observed to decrease with increasing ambient or enclosure humidity for both analytes (Figure 3c and d). The relative abundance of molecular adduct ions from limonene was lower than nicotine at a given humidity value, and the increase in fragmentation observed in the enclosure was more pronounced for limonene. The slope of the ambient humidity dependence was negligible below 4 g/m^3 for both analytes.

Unlike other analytes studied here, safrole introduced via GC did not produce MH^+ . FAPA mass spectra of safrole contained $[M - H]^+$, M^{++} , and fragment ions (Online Resource 7). The fragmentation of molecular adduct ions decreased as ambient and enclosure humidity increased (Figure 3e), isolating the humidity effect of changing average reagent proton affinity for an analyte ionized by proton abstraction and not proton transfer. Fragmentation in the enclosure appeared approximately equal to results at ambient humidity below 8 g/m^3 , but at greater ambient humidity the safrole fragmentation decreased more sharply.

The fragmentation dependence on humidity was approximately linear for most analytes, though sometimes

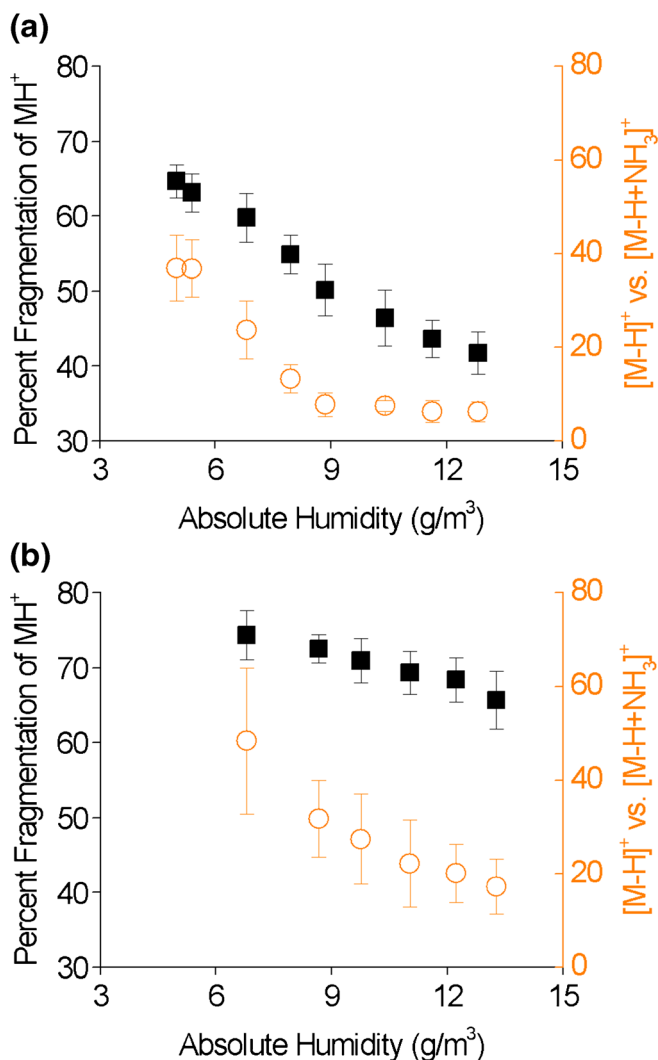


Figure 4. DART signal from HMTD with variation of enclosure humidity at discharge gas temperature (a) 150°C and (b) 350°C , and $30\text{--}31^\circ\text{C}$ enclosure temperature, shown as percent fragmentation of protonated molecule (■) and ratio of protonated and ammoniated dialdehyde adducts (orange ○) (\pm one SD)

characterized by trend plateaus or inflection points. The change in slope at low and high ambient humidity values on several curves suggests non-linear relationships over a wider range than was observable under ambient conditions in the laboratory or with the enclosure, which is consistent with the observations of Sunner et al. [29], and Jost and coworkers [30]. The elevated temperature of the enclosure also tended to produce lower slopes similar to trends at lower ambient humidity ranges because the additional thermal energy increased fragmentation overall. Variation in the relative abundance of molecular adduct ions and fragment ions with ambient humidity was significant for all analytes except propazine (Online Resource 8). The more constant fragment ion relative abundance of propazine and the highly linear fragmentation dependence on humidity reflect the fact that propazine was the only analyte studied with a single molecular adduct ion.

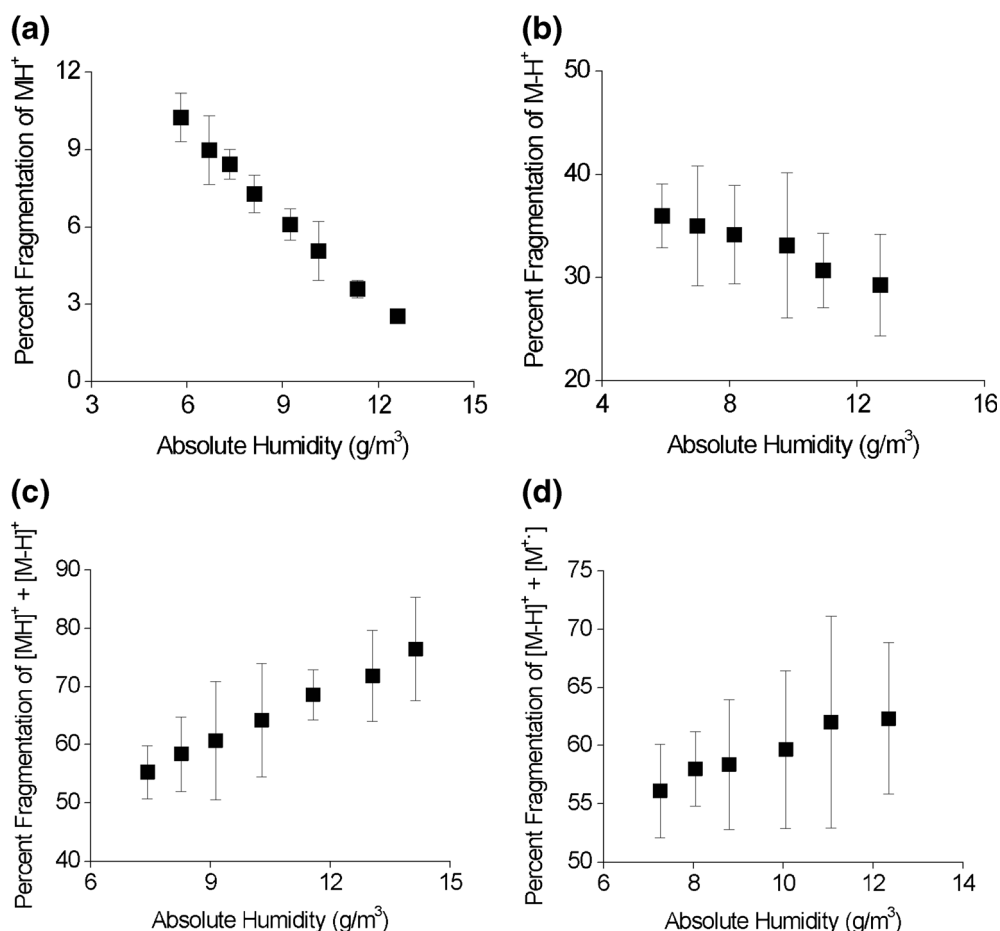


Figure 5. DART signal from (a) propazine, (b) nicotine, (c) limonene, and (d) safrole using 150°C discharge gas with variation of enclosure humidity at 28–33°C, shown as percent fragmentation of protonated molecule (a), (b); protonated molecule and net deprotonated molecule (c); and net deprotonated molecule and molecular ion (d) (\pm one SD)

DART Mass Spectra of Analytes as a Function of Humidity

DART ambient mass spectra of paper-deposited HMTD contained the same ions as FAPA ambient mass spectra. Also observed were two abundant adducts of a dialdehyde form of HMTD produced by peroxide bond cleavage [31], protonated for a net molecular formula of $[M - H]^+$ [32], and ammoniated for a net molecular formula of $[M - H + NH_3]^+$ [33]. The MH^+ and fragment ions at m/z 179 and 145 were consistently more abundant than the m/z 88 radical fragment ion. DART mass spectra of HMTD were also acquired using the enclosure. The humidity was varied at both 150°C and 350°C discharge gas temperatures (Figure 4), profiling analyte spectra at two temperature regimes similar to the way FAPA experiments were performed at ambient and elevated temperatures. MH^+ fragmentation decreased with increasing humidity, but the abundance of $[M - H]^+$ decreased relative to $[M - H + NH_3]^+$ abundance. Both trends had a lower slope at 350°C discharge gas than 150°C, similar to results from FAPA analysis.

DART is typically operated with the minimum temperature necessary to rapidly desorb targeted analytes, and the remainder of analyses were performed in the enclosure with 150°C

discharge gas. Each DART mass spectrum contained molecular adduct ions similar to FAPA but generally with reduced fragmentation, likely due to the removal of excited-state species other than metastable helium [6]. Ferrocene adduct ion fragmentation by DART was absent and is not discussed. Propazine deposited on paper was the only analyte studied by DART that produced a single form of molecular adduct ion, and MH^+ fragmentation decreased with increasing humidity (Figure 5a). Nicotine introduced to the ionization region by GC produced MH^+ and $[M - H]^+$, but with large signal relative standard deviation (RSD) only the net deprotonated molecule fragmentation could confidently be said to have changed due to humidity (Figure 5b). Limonene also produced MH^+ and $[M - H]^+$, and changes in humidity changed the percent fragmentation of both molecular adduct ions (Figure 5c). In the most substantial difference between DART and FAPA results, DART of limonene demonstrated increased fragmentation with increasing humidity. The particular complexity of limonene mass spectra made it difficult to determine which species or mechanisms reversed the trend, but results with FAPA of ferrocene suggest that hydration of limonene fragment ions may be dominant with DART. Fragmentation of $[M - H]^+$ and M^{++} from safrole also showed a positive slope but did not

increase outside the bounds of standard deviation error bars over the studied humidity range (Figure 5d). Unlike other DART analytes producing multiple molecular adduct ions, neither saffrole nor nicotine showed significant change in ion relative abundance with humidity (Online Resource 9). More significant humidity effects for analytes might be observed over a wider humidity range and with lower RSD values similar to FAPA measurements. The slope of humidity effects on fragmentation in DART mass spectra was particular to the analyte, likely because of unique proton affinity values and reaction pathways, as with FAPA. Humidity effects on DART spectra were less observably significant than effects on FAPA spectra due to a lower degree of initial fragmentation and higher signal and spectral variability. DART control of discharge gas temperature can stabilize humidity effects at higher temperatures, depending on the analyte.

Conclusions

The demonstrated change in protonated water cluster population with humidity (and thus average reagent proton affinity) directly affects analyte fragmentation. Increasing the ambient or discharge gas temperature lowers the humidity effect with both ion sources but also causes more fragmentation. Humidity effects would likely be even more significant with post-plasma ADI sources that operate at lower temperatures, such as the low temperature plasma probe [11]. High molecular adduct ion fragmentation at low humidity and high temperature could be detrimental to trace detection and MS/MS applications, whereas the spectral variance might limit library searching or ion-ratio confirmations. Although it might be possible to calibrate for humidity where the effects are shown to be linear and the ionization follows a single mechanism (as with propazine), current libraries do not record humidity/temperature of post-plasma spectra [34].

In the absence of a source enclosure or sweep gas, a commercialized ADI system like DART may specify an operation range for humidity. However, like the effects of background gas-phase contaminants familiar to ambient ionization users, circumstances frequently prevent control of ambient humidity. Laboratory air in any facility is susceptible to humidity variation, particularly with season. Results have indicated that even a narrow operating range of humidity may produce enough variation (e.g., changing the base peak) to hinder reproducibility for quantitation or mass spectra library matching. Significant changes in molecular adduct ion signal abundance especially impair trace detection and quantitation or MS/MS ion statistics. One solution is to indirectly control humidity by elevating discharge temperature so that humidity effects are diminished without also causing excessive fragmentation [24]. However, differing energetics would require empirical study to find an optimal temperature balance for each analyte, a complication to the rapid, simple analyses that characterize post-plasma ADI sources. Humidity can instead be directly controlled in a source area without raising temperature and risking

increased fragmentation. Adding a controllable amount of water vapor, rather than drying the ionization region with elevated temperatures, stabilizes post-plasma ADI signal and lowers or eliminates molecular adduct ion fragmentation for most compounds.

Acknowledgments

The authors thank Michael Malito of Nova Research, Inc. for assistance designing the source enclosure; the Gary M. Hieftje lab of Indiana University for providing the FAPA source; Jon Wong of the FDA Center for Food Safety and Applied Nutrition for providing propazine; and Lauryn DeGreeff-Silk of the Naval Research Laboratory for preparing the HMTD solution. Funding for this project was provided by the Office of Naval Research (ONR) through the Naval Research Laboratory's Basic Research Program.

References

1. Van Berkel, G.J., Pasilis, S.P., Ovchinnikova, O.: Established and emerging atmospheric pressure surface sampling/ionization techniques for mass spectrometry. *J. Mass Spectrom.* **43**, 1161–1180 (2008)
2. Huang, M.-Z., Cheng, S.-C., Cho, Y.-T., Shiea, J.: Ambient ionization mass spectrometry: a tutorial. *Anal. Chim. Acta* **702**, 1–15 (2011)
3. Huang, M.-Z., Yuan, C.-H., Cheng, S.-C., Cho, Y.-T., Shiea, J.: Ambient ionization mass spectrometry. *Annu. Rev. Anal. Chem.* **3**, 43–65 (2010)
4. Albert, A., Shelley, J.T., Engelhard, C.: Plasma-based ambient desorption/ionization mass spectrometry: state-of-the-art in qualitative and quantitative analysis. *Anal. Biochem.* **406**, 6111–6127 (2014)
5. Hiraoka, K., Fujimaki, S., Kambara, S., Furuya, H., Okazaki, S.: Atmospheric-pressure Penning ionization mass spectrometry. *Rapid Commun. Mass Spectrom.* **18**, 2323–2330 (2004)
6. Cody, R.B., Laramee, J.A., Durst, H.D.: Versatile new ion source for the analysis of materials in open air under ambient conditions. *Anal. Chem.* **77**, 2297–2302 (2005)
7. Na, N., Zhao, M., Zhang, S., Yang, C., Zhang, X.: Development of a dielectric barrier discharge ion source for ambient mass spectrometry. *J. Am. Soc. Mass Spectrom.* **18**, 1859–1862 (2007)
8. Na, N., Zhang, C., Zhao, M., Zhang, S., Yang, C., Fang, X., Zhang, X.: Direct detection of explosives on solid surfaces by mass spectrometry with an ambient ion source based on dielectric barrier discharge. *J. Mass Spectrom.* **42**, 1079–1085 (2007)
9. Ratcliffe, L.V., Rutten, F.J.M., Barrett, D.A., Whitmore, T., Seymour, D., Greenwood, C., Aranda-Gonzalvo, Y., Robinson, S., McCoustra, M.: Surface analysis under ambient conditions using plasma-assisted desorption/ionization mass spectrometry. *Anal. Chem.* **79**, 6094–6101 (2007)
10. Andrade, F.J., Shelley, J.T., Wetzel, W.C., Webb, M.R., Gamez, G., Ray, S.J., Hieftje, G.M.: Atmospheric pressure chemical ionization source. 1. Ionization of compounds in the gas phase. *Anal. Chem.* **80**, 2646–2653 (2008)
11. Harper, J.D., Charipar, N.A., Mulligan, C.C., Zhang, X., Cooks, R.G., Ouyang, Z.: Low-temperature plasma probe for ambient desorption ionization. *Anal. Chem.* **80**, 9097–9104 (2008)
12. Wiley, J.S., Shelley, J.T., Cooks, R.G.: Handheld low-temperature plasma probe for portable "point-and-shoot" ambient ionization mass spectrometry. *Anal. Chem.* **85**, 6545–6552 (2013)
13. Shelley, J.T., Wiley, J.S., Chan, G.C.Y., Schilling, G.D., Ray, S.J., Hieftje, G.M.: Characterization of direct-current atmospheric-pressure discharges useful for ambient desorption/ionization mass spectrometry. *J. Am. Soc. Mass Spectrom.* **20**, 837–844 (2009)
14. Chan, G.C.Y., Shelley, J.T., Wiley, J.S., Engelhard, C., Jackson, A.U., Cooks, R.G., Hieftje, G.M.: Elucidation of reaction mechanisms responsible for afterglow and reagent-ion formation in the low-temperature plasma probe ambient ionization source. *Anal. Chem.* **83**, 3675–3686 (2011)

15. Cody, R.B.: Observation of molecular ions and analysis of nonpolar compounds with the direct analysis in real time ion source. *Anal. Chem.* **81**, 1101–1107 (2009)
16. Song, L., Gibson, S.C., Bhandari, D., Cook, K.D., Bartmess, J.E.: Ionization mechanism of positive-ion direct analysis in real time: a transient microenvironment concept. *Anal. Chem.* **81**, 10080–10088 (2009)
17. Gross, J.H.: *Ambient Mass Spectrometry*. In: *Mass Spectrometry-A Textbook*, 2nd edn. Springer, Heidelberg (2011)
18. Hardware and Network Installation Manual For DART SVP Source and Controllers. Revision 5, Document 7.5.031 ed. Available at: www.ionsense.com. http://www.ionsense.com/pdfs/SVPHardwareandNetworkInstallationManual_Rev5_7.5.031.pdf. Accessed 14 Sept 2015
19. Zehentbauer, G., Krick, T., Reineccius, G.A.: Use of humidified air in optimizing APCI-MS response in breath analysis. *J. Agric. Food Chem.* **48**, 5389–5395 (2000)
20. Portoles, T., Mol, J.G.J., Sancho, J.V., Hernandez, F.: Advantages of atmospheric pressure chemical ionization in gas chromatography tandem mass spectrometry: pyrethroid insecticides as a case study. *Anal. Chem.* **84**, 9802–9810 (2012)
21. Matysik, S., Schmitz, G., Bauer, S., Kiermaier, J., Matysik, F.M.: Potential of gas chromatography-atmospheric pressure chemical ionization-time-of-flight mass spectrometry for the determination of sterols in human plasma. *Biochem. Bioph. Res.* **446**, 751–755 (2014)
22. Wachsmuth, C.J., Dettmer, K., Lang, S.A., Mycielska, M.A., Oefner, P.J.: Continuous water infusion enhances atmospheric pressure chemical ionization of methyl chloroformate derivatives in gas chromatography coupled to time-of-flight mass spectrometry-based metabolomics. *Anal. Chem.* **86**, 9186–9195 (2014)
23. Newsome, G.A., Ackerman, L.K., Johnson, K.J.: Humidity affects relative ion abundance in direct analysis in real time mass spectrometry of hexamethylene triperoxide diamine. *Anal. Chem.* **86**, 11977–11980 (2014)
24. Orejas, J., Pfeuffer, K.P., Ray, S.J., Pisonero, J., Sanz-Medel, A., Hieftje, G.M.: Effect of internal and external conditions on ionization processes in the FAPA ambient desorption/ionization source. *Anal. Biochem.* **406**, 7511–7521 (2014)
25. Hardy, R.: ITS-90 formulations for vapor pressure, frost point temperature, dew point temperature, and enhancement factors in the range –100 to +100 C. *Papers and Abstracts of the Third International Symposium on Humidity and Moisture* **1**, 214–222 (1998)
26. Available at: <http://www.humidity-calculator.com>. Accessed 14 Sept 2015
27. Shelley, J.T., Wiley, J.S., Hieftje, G.M.: Ultrasensitive ambient mass spectrometric analysis with a pin-to-capillary flowing atmospheric-pressure afterglow source. *Anal. Chem.* **83**, 5741–5748 (2011)
28. Kawai, Y., Yamaguchi, S., Okada, Y., Takeuchi, K., Yamauchi, Y., Ozawa, S., Nakai, H.: Reactions of protonated water clusters $H+(H_2O)(n)$ ($n = 1-6$) with dimethylsulfoxide in a guided ion beam apparatus. *Chem. Phys. Lett.* **377**, 69–73 (2003)
29. Sunner, J., Nicol, G., Kebarle, P.: Factors determining relative sensitivity of analytes in positive mode atmospheric pressure ionization mass spectrometry. *Anal. Chem.* **60**, 1300–1307 (1988)
30. Jost, C., Sprung, D., Kenntner, T., Reiner, T.: Atmospheric pressure chemical ionization mass spectrometry for the detection of tropospheric trace gases: the influence of clustering on sensitivity and precision. *Int. J. Mass Spectrom.* **223**, 771–782 (2003)
31. Wierzbicki, A., Salter, E.A., Cioffi, E.A., Stevens, E.D.: Density functional theory and X-ray investigations of P- and M-hexamethylene triperoxide diamine and its dialdehyde derivative. *J. Phys. Chem. A.* **105**, 8763–8768 (2001)
32. Tamiri, T., Zitrin, S.: *Explosives: Analysis*. In: Siegel, J.A., Saukko, P.J. (eds.) *Encyclopedia of Forensic Sciences*, 2nd edn. Elsevier, Waltham (2013)
33. Marr, A.J., Groves, D.M.: Ion mobility spectrometry of peroxide explosives TATP and HMTD. *Int. J. Ion. Mobil. Spectrom.* **6**, 59–62 (2003)
34. Available at: <http://chemdata.nist.gov/dokuwiki/doku.php?id=chemdata:dart-library>. Accessed 14 Sept 2015